High-throughput first-principles search for new ferroelectrics

Kevin F. Garrity[*]

Material Measurement Laboratory, National Institute of Standards and Technology, Gaithersburg, Maryland 20899, USA

We use a combination of symmetry analysis and high-throughput density functional theory calculations to search for new ferroelectric materials. We use two search strategies to identify candidate materials. In the first strategy, we start with nonpolar materials and look for unrecognized energy-lowering polar distortions. In the second strategy, we consider polar materials and look for related higher symmetry structures. In both cases, if we find new structures with the correct symmetries that are also close in energy to experimentally known structures, then the material is likely to be switchable in an external electric field, making it a candidate ferroelectric. We find 16 candidate materials, with a variety of properties that are rare in typical ferroelectrics, including large polarization, hyperferroelectricity, antiferroelectricity, and multiferroism.

I. INTRODUCTION

Ferroelectrics, which are materials that have a ground-state polar phase that can be switched to a symmetry-equivalent structure by the application of an external electric field, have been studied and used in applications for many years. Much of the attention on ferroelectrics has focused on prototypical examples from the perovskite oxides, like $PbTiO_3$ and $BiFeO_3$. However, in recent years, there has been a renewed theoretical and experimental interest in discovering and understanding the properties of new ferroelectric materials [1–14]. These new materials have shown a variety of new or rare behaviors, including hybrid improper ferroelectricity, hyperferroelectricity, topological defects/domain walls, etc. In addition, there is interest in and need for ferroelectrics with improved functionality for various applications, including magnetoelectrics, Pb-free piezoelectrics, room temperature multiferroics, solar energy converters, silicon compatible ferroelectrics, ferroelectric catalysts, etc. [15–20].

High-throughput first-principles density functional theory (DFT) calculations have been used increasingly in recent years as a tool for materials discovery and screening, and large databases of electronic structure calculations of experimentally known materials exist [21–26]. DFT calculations using semilocal functionals are generally reliable tools for computing ground-state properties and the energy differences between closely related phases, which is the primary screening tool needed to identify ferroelectrics. The main obstacle to finding new ferroelectric materials computationally is identifying the relevant polar and nonpolar structures to consider. Any insulator known experimentally to have both a polar and a nonpolar phase has likely already been recognized as a potential ferroelectric, necessitating a search for new structures of known compounds. For a single family of materials like the perovskites, it may be possible to systematically consider all possible distortions of a certain type, organized

by symmetry considerations [27–29]. However, searching all insulating compounds for every possible distorted phase is too computationally demanding to attempt systematically, as any polar subgroup of a reference structure is allowed in general.

In this work, we employ two strategies to identify new ferroelectrics, which we apply to a much larger range of materials than related previous searches [1,10,14,30–37]. In the first strategy, aimed at finding proper ferroelectrics, we start with a list of experimentally known nonpolar transition metal oxides, nitrides, and sulfides, and we perform a Γ-point phonon calculation, looking for materials with unstable polar modes. In order to reduce the computational cost of this step, we reuse phonon calculations from our earlier study of transition metal thermoelectricity [38], and we supplement this list with additional calculations of materials with small unit cells. After identifying materials with unstable polar distortions, we proceed to look for the ground-state structure, including possible nonpolar distortions. If the ground state is polar, then the material is a candidate ferroelectric.

In the second strategy, we begin instead with a list of materials already known to be polar but not known to be switchable in an external electric field. We attempt to identify switchable materials by using a symmetry search algorithm [39] and adjusting the tolerance factor systematically to allow the algorithm to identify possible higher symmetry structures that are related to the polar ground state. We then calculate the energy of these new structures, and if they are close in energy to the polar structure, the materials are likely to be switchable [1]. An advantage to both of our search strategies is that they are not limited to generating previously observed structure types, allowing us to consider new mechanisms for creating polar distortions. Furthermore, all of the materials we consider have been synthesized experimentally in previous works.

In the remainder of this work, we will detail our search strategy, identify candidate ferroelectrics, and discuss some of their interesting properties. We find materials with unusual chemistry for ferroelectrics, as well as potentially useful properties that include strong polarization, magnetism, hyperferroelectricity, and antiferroelectricity. In addition, we rediscover

———
*kevin.garrity@nist.gov

024115-1

and identify the missing structures of two materials that were previously studied as ferroelectrics but have not been fully characterized. Full structural details of our candidate materials can be found in the Supplemental Material [40].

II. METHODS

A. First-principles calculations

We perform first-principles DFT calculations [41,42] with a plane-wave basis set as implemented in QUANTUM ESPRESSO [43] and using the GBRV high-throughput ultrasoft pseudopotential library [44,45]. We use a plane-wave cutoff of 40 Ryd for band structure calculations and 45–50 Ryd for phonon calculations [46]. For Brillouin zone integration, we use a Γ-centered grid with a density of 1500 k points per atom.

We use the PBEsol exchange-correlation functional [47], which provides more accurate lattice constants and phonon frequencies than other generalized gradient approximation functionals (except for $CuBiW_2O_8$, see Sec. III D). We perform phonon calculations using DFT perturbation theory [48], and polarization calculations with the Berry phase method [49]. We use PYMATGEN [39] to manipulate files from the Inorganic Crystal Structure Database (ICSD) to set up the initial structures for relaxation. We relax each structure several times to ensure consistency between the basis set and the final structure, with a force tolerance of 0.001 Ry/Bohr, an energy tolerance of 1×10^{-4} Ry, and a stress tolerance of 0.5 Kbar. For phonon calculations, we decrease the force tolerance to 5×10^{-5} Ry/Bohr.

B. Search strategy

To identify ferroelectrics, we look for materials that are (a) insulating, (b) have a polar ground state, and (c) have a higher symmetry reference structure that is close in energy to the polar structure, which we take as an indication the material is likely to be switchable in an external electric field. Some examples of this energy difference for known ferroelectrics include $PbTiO_3$ (20 meV/atom), $Ca_3Ti_2O_7$ (40 meV/atom), and ZrO_2 (16 meV/atom) [5,9]. Of course, in real ferroelectrics, the switching proceeds via a combination of domain wall nucleation and motion, and does not correspond directly to the first-principles energy difference; however, a small energy difference has proven to be a useful indicator of whether a material is likely to be switchable [1,2,5,30,32–34,50].

In our first search strategy, we start with materials where a high symmetry nonpolar structure is known to exist, and we search for possible energy-lowering polar distortions. Because our calculations are done at zero temperature while most structure determinations are done at room temperature, if an energy-lowering polar distortion is found, and potential competing phases are ruled out, it should be possible to reach the polar phase experimentally by lowering the temperature. A second possibility is that a material with a small polar distortion could have been misidentified as nonpolar during an experimental structure determination.

At zero temperature, some degrees of freedom of the high symmetry structure are not at local minima, and the structure is only found on average due to thermal fluctuations at higher temperatures. However, analysis of ferroelectrics based on

zero temperature distortions of the unstable high symmetry phase is widely used to gain understanding of the possible low symmetry phases, and our main purpose is to identify possible low symmetry phases [51,52]. Full relaxations are necessary to determine the low energy structures.

In this strategy, the initial screening step is to perform a Γ-point phonon calculation, which we did for 267 transition metal oxides, nitrides, and sulfides. A Γ-point phonon calculation is sufficient to eliminate materials without energy-lowering polar distortions, but further calculations are necessary to find the ground-state structure. This screening step also will generally eliminate improper ferroelectrics. We identified 90 compounds with unstable modes at Γ, although some of these distortions were nonpolar. After excluding known ferroelectrics and materials with known nonpolar distortions, we proceeded to search for the ground-state structure.

This search consisted of first calculating the full phonon dispersion of the material, and then freezing in finite amounts of each unstable phonon eigenvector, as well as pairs of eigenvectors, into supercells that correspond to points in the Brillouin zone with unstable modes. For unstable modes away from Γ, this requires increasing the size of the unit cell to accommodate antipolar distortions. We then relax the resulting structures [14,53,54]. For systems with many unstable modes, which could have ground states consisting of complicated distortion patterns, we supplemented this searching with a random search strategy [54]. To perform a random search, we take a supercell, freeze in small random distortions, and relax. For most materials, we found that after a set of 10 random relaxations in a given supercell, the same low energy structures repeated several times, and we terminated the search. There is no symmetry constraint on our ground structure search, and we use a symmetry search algorithm [39] to determine the final symmetry.

After this search process, if a material has a polar ground state, then the material is a candidate ferroelectric. In addition, if the material has competing polar and antipolar phases, then the material is a candidate antiferroelectric [2,50]. In the top rows of Table I, we present six candidate ferroelectrics discovered with this strategy.

In our second search strategy, we considered a list about 2750 compounds from the ICSD with small unit cells and polar ground states. For each compound, we used the symmetry detection algorithm of pymatgen [39] and varied the tolerance factor from 10^{-6} to 3, looking for related structures with higher symmetry that have otherwise reasonable structures (e.g., no atoms on top of each other). For compounds where new structures were found, we then relaxed both the experimentally known polar structure and any new structures. In most cases, the new structures were very high energy. For example, in many structures with covalent bonds, the new structures had broken bonds and were unrealistic. In addition, we found a small number of compounds in the opposite situation, where the polar phase relaxed to a nonpolar structure. These materials were either misidentified as polar experimentally, or are not well described by the PBEsol functional.

However, in addition to those cases, we found 10 compounds that have a low but nonzero energy difference between their polar and nonpolar structures, making them candidate ferroelectrics. In this case, we do not search for possible

TABLE I. Data on candidate ferroelectrics, found by starting from high-symmetry (top) and low-symmetry (bottom) structures. The second and third columns are space groups of the high- and low-symmetry structures, column four is the energy difference in meV/atom, and the last column is the polarization in $\mu C/cm^2$.

Composition	High-symmetry space group	Polar space group	ΔE (meV/atom)	Polarization ($\mu C/cm^2$)
$SrNb_6O_{16}$	$Amm2$	Cm	5.5	7
$NaNb_6O_{15}F$	$Amm2$	Cm	9.5	6
$RbCa_2Nb_3O_{10}$	$P4/mmm$	Pc	46.6	23
$BaBi_2Ta_2O_9$	$I4/mmm$	$Cmc2_1$	15.7	37
$LiScAs_2O_7$	$C2$	$P1$	1.6	7
YSF	$P6_3/mmc$	$P6_3mc$	11.1	1.2
$CuBiW_2O_8$	$P\bar{1}$	$P1$	0.3	6
$PbGa_2O_4$	$P\bar{6}2c$	$Ama2$	108	23
$PbAl_2O_4$	$P\bar{6}2c$	$Ama2$	75	18
LiV_2O_5	$Pmmn$	$Pmn2_1$	0.4	9
$NaVO_2F_2$	$P2_1/m$	$P2_1$	0.3	18
SbW_2O_6	$P2_1/c$	$P2_1$	4.4	21
V_2MoO_8	$Cmmm$	$Cmm2$	84	108
Zn_2BrN	$Pnma$	$Pna2_1$	1.3	1.4
Zn_2ClN	$Pnma$	$Pna2_1$	2.4	1.5
$AlAgO_2$	$Pnma$	$Pna2_1$	71	0.2

competing phases unless they are already known to exist experimentally. We list them in the second section of Table I, and we discuss a few interesting cases below.

III. RESULTS

First, we note that after doing our analysis, we discovered that $BaBi_2Ta_2O_9$ and related materials with Sr and Ca have previously been studied as a ferroelectrics [55]. However, only a pseudotetragonal twinned version of the polar structure of $BaBi_2Ta_2O_9$ had been determined, explaining why it did not show up in our database search as a polar. This material has a layered structure that consists of perovskite-like $BaTaO_3$ layers separated by BiO layers, and these layers shift relative to each other in-plane, resulting in a relatively large polarization. Re-identifying a known ferroelectric gives us confidence in the utility of our computational methodology.

Sb_2WO_6 is a second example of a previously known (anti-)ferroelectric/ferroelastic [56] that our procedure rediscovered. In this case, the polar structure was previously characterized experimentally, and we have provided new information about the nonpolar phase.

In the rest of this section we briefly discuss the properties of many of our new candidate ferroelectrics.

A. $SrNb_6O_{16}$ and $NaNb_6O_{15}F$

$SrNb_6O_{16}$ [57], shown in Fig. 1, and the closely related $NaNb_6O_{15}F$, have a variety of notable properties. We will concentrate on $SrNb_6O_{16}$, which has a high symmetry structure consisting of layers of Nb_6O_{10} spaced by SrO_6 layers. The material has a nonreversible in-plane polarization, but the switchable portion of the polarization consists of out-of-plane buckling in the Nb_6O_{10} layers. Because of the large number of atoms in the unit cell, there are a variety of unstable
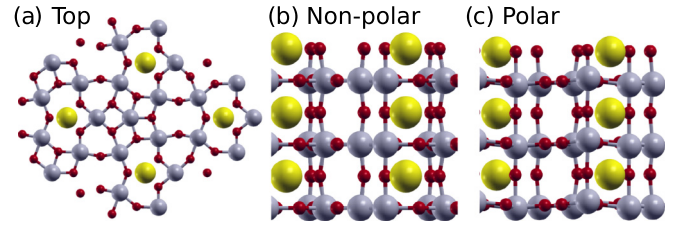

FIG. 1. Atomic positions of $SrNb_6O_{16}$. (a) Top view, (b) side view of nonpolar structure, and (c) side view of polar structure. The Sr are the large yellow atoms, the Nb are the medium gray atoms, and the O are the small red atoms.

polar and nonpolar bucklings. $SrNb_6O_{16}$ has anomalously large Born effective charges in the z direction of 9 to 11 on the Nb atoms and -7 to -9 on the O atoms. In the xy plane, the effective charges are much lower, and Sr has an effective charge of 2.4. Similar anomalous effective charges are well known in the perovskite oxides [51] but are not present in many alternative ferroelectrics [4,6].

Despite these enormous effective charges, $SrNb_6O_{16}$ is actually a candidate hyperferroelectric [4], a very rare category of proper ferroelectrics with instabilities of both the longitudinal optic (LO) and transverse optic (TO) modes, as shown in Table II. These instabilities correspond to unstable polar modes under both zero electric field ($\mathbf{E}=0$) and zero displacement field ($\mathbf{D}=0$) boundary conditions. The polar distortions of normal ferroelectrics are stable under $\mathbf{D}=0$ boundary conditions.

We were initially very surprised to find a hyperferroelectric with large effective charges, as the energetic cost of producing long-range electric fields is proportional to $(Z^*)^2/\epsilon$, where ϵ is the electronic dielectric constant and Z^* is the effective charge [4,58]. $SrNb_6O_{16}$ avoids this by having three different unstable polar modes that can mix with each other, producing modes that are still polar, but with much smaller mode effective charges under $\mathbf{D}=0$ boundary conditions, as detailed in Table II. Hopefully, hyperferroelectric oxides similar to $SrNb_6O_{16}$ are more common than previously thought, especially as hyperferroelectrics have potential applications as single layer ferroelectric devices. Further work must be done to understand the $\mathbf{D}=0$ ground state in this material [59].

TABLE II. Unstable LO and TO phonon frequencies and mode effective charges in $SrNb_6O_{16}$ at Γ. The first two columns are the frequency in cm^{-1} and the mode Born effective charge of the LO modes; the second two columns are the same but for the TO modes. There is one antipolar mode with zero mode effective charge that is unaffected by electrostatic boundary conditions.

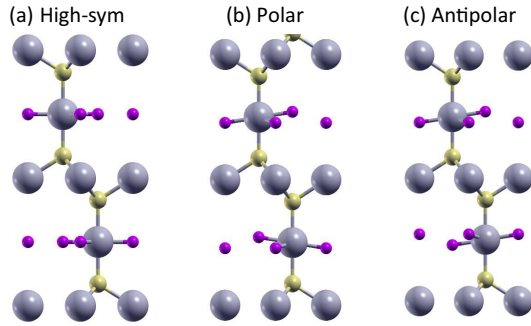| Mode number	LO frequency (cm^{-1})	LO Mode Z^*	TO Frequency (cm^{-1})	TO Mode Z^*
1	$176i$	21.8	$139i$	0.23
2	$138i$	5.9	$128i$	0
3	$128i$	0	$85i$	1.2
4	$44i$	10.2	$29i$	0.32

FIG. 2. Atomic positions of YSF. (a) High symmetry, (b) polar, and (c) antipolar phases. Y are the large gray atoms, S are the medium yellow atoms, and F are the small purple atoms.

B. YSF

Another compound with interesting behavior is YSF [60]. As shown in Fig. 2, YSF consists of alternating layers of YF_2 and YS_2, and the YF_2 layers display an energy lowering out-of-plane buckling that is locally antipolar. However, due to longer range interactions with the YS_2 layers, this buckling is actually weakly polar [61,62], and the material can become either polar or antipolar depending on how the buckling in adjacent YF_2 layers is aligned. We find that the polar phase of YSF is nominally lower in energy than the antipolar version, but the energy difference is less than 0.1 meV/atom, making YSF a potential antiferroelectric as well. In fact, given the weak coupling between layers, there are likely a high number of layer stackings with nearly degenerate energies, which could then be ordered by an external field.

C. LiScAs₂O₇

As shown in Fig. 3, the polar distortion of $LiScAs_2O_7$ consists almost entirely of the Li atom off-centering, likely due to its small size. By moving off-center, the Li atom increases its coordination from fourfold to fivefold, while the four shortest Li-O bonds average 2.12 Å in either structure. This polar distortion pattern of Li moving off-center is similar to LiV_2O_5, as discussed below.
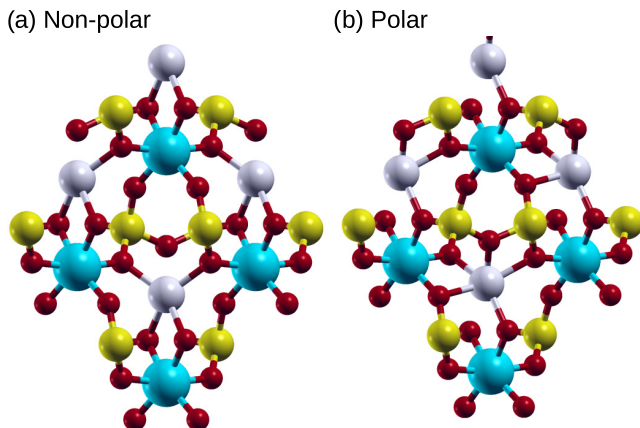

FIG. 3. Atomic positions of $LiScAs_2O_7$. (a) High symmetry and (b) polar phases. Li are the light gray atoms, As are the medium yellow atoms, Sc are the large cyan atoms, and O are the small red atoms.
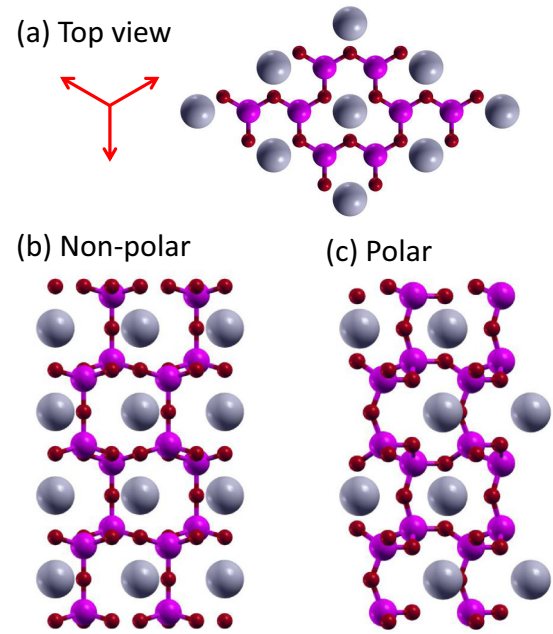

FIG. 4. Atomic positions of $PbAl_2O_4$. (a) and (b) Top and side view of nonpolar phase. (c) Side view of polar phase. Red arrows in (a) show three equivalent polarization directions. Large gray atoms are Pb, medium magenta atoms are Al, and small red atoms are O.

D. CuBiW₂O₈

The compound $CuBiW_2O_8$, as well as the five related materials listed in the ICSD with structure type $CuNb(WO_4)_2\beta$, is listed as having no symmetry in the ICSD [63]. However, according to PBEsol calculations, $CuBiW_2O_8$ and the related $CuYW_2O_8$ relax to a higher symmetry structure with only inversion symmetry, suggesting that these materials do not have a polar phase. We were surprised to find so many materials possibly misidentified, so we performed LDA [64] calculations to verify our result. We instead found that $CuBiW_2O_8$ (but not $CuYW_2O_8$) does have polar distortion, with a very small energy difference and polarization, as listed in Table I. This functional-dependent behavior is the opposite of the typical behavior of LDA and GGA functionals, where GGA tends to overestimate polar distortions, while LDA underestimates. Further work may be necessary to reveal whether this class of materials is really polar/ferroelectric.

E. PbGa₂O₄ and PbAl₂O₄

The pair of compounds $PbGa_2O_4$ and $PbAl_2O_4$ consist of $(Al,Ga)O_4$ tetrahedra separated by Pb atoms [65], as shown for $PbAl_2O_4$ in Fig. 4. Their high symmetry structures have a threefold rotation axis, and the polarization, which is due to a collective tilting of the tetrahedra, points in one of three equivalent in-plane directions, as shown in Fig. 4(a). The structure with 180° reversed polarization does not have the same energy, which can be understood by examining the symmetry invariant free energy of the two-dimensional Γ_5 distortion up to fourth order:

$$F = c_2\left(\Gamma_{5a}^2 + \Gamma_{5b}^2\right) + c_3\left(\Gamma_{5a}^3 - 3\Gamma_{5a}\Gamma_{5b}^2\right)$$
$$+ c_4\left(\Gamma_{5a}^4 + 2\Gamma_{5a}^2\Gamma_{5b}^2 + \Gamma_{5b}^4\right). \quad (1)$$
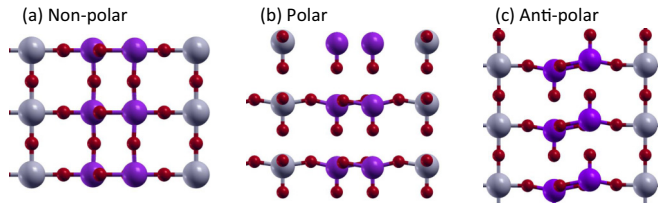
FIG. 5. (a) High-symmetry, (b) polar, and (c) antipolar phases of V_2MoO_8. The medium gray and magenta atoms are Mo and V, respectively, and the small red atoms are O.

FIG. 6. (a) Nonpolar and (b) polar phases of LiV_2O_5. The red arrow in (b) highlights off-centering of Li. Light gray atoms are Li, magenta atoms are V, and small red atoms are O.

In this notation the ground-state polar structure corresponds to $\Gamma_{5a} > 0$, $\Gamma_{5b} = 0$, and the constants c_2 and c_3 are negative, while c_4 is positive. Unlike a typical proper ferroelectric, there is a third-order term, which explains why the structure with reversed polarization is inequivalent.

The reversed polarization direction structure is only 9 meV/atom higher in energy higher than the ground state for $PbAl_2O_4$. This intermediate structure represents the transition state between two stable polarization directions, which we confirm with nudged elastic band calculations [66]. Therefore, it is possible to switch the polarization of $PbGa_2O_4$ and $PbAl_2O_4$ by rotating it 120° while avoiding the higher energy high-symmetry structure, resulting in a barrier that is eight times lower in energy than the naive switching path. In effect, there is very little barrier to rotating the polarization direction any direction in-plane, even though reducing the polarization to zero results in a high energy state. This combination could allow for a high Curie temperature ferroelectric material.

F. V_2MoO_8

The layered structure of V_2MoO_8 [67] is interesting for possible applications because it has an enormous polarization of 108 $\mu C/cm^2$, comparable to the largest polarizations in perovskites [68]. Both the V and the Mo atoms are located in distorted oxygen octahedra, and all three ions displace in the same direction in the polar structure. This combined distortion of ions, all with large nominal charges, is what results in the enormous polarization in this material.

As shown in Fig. 5, this material actually has three low energy structures: the high-symmetry phase, the polar phase, and an antipolar phase [69,70], which is also seen experimentally and which is 48 meV/atom lower in energy than the polar phase. In the antipolar phase, the V atoms still have large polar distortions, but they distort in opposite directions, and the Mo remains in the center of its octahedron. Because the ground state of V_2MoO_8 is antipolar with a competing polar phase, this material is better characterized as a candidate antiferroelectric. The very large polarization of the polar phase of this material could make V_2MoO_8 useful in applications like antiferroelectric energy storage, where a large polarization jump is desirable.

Also, we note that due to the Mo(+6) and V(+5) ions in the structure, this material has a relatively small band gap of only 0.95 eV according to our calculations. Although quantitatively predicting the band gap of transition metal oxides is difficult, the combination of an oxide with a large polarization and a small gap are potentially useful for solar power applications.
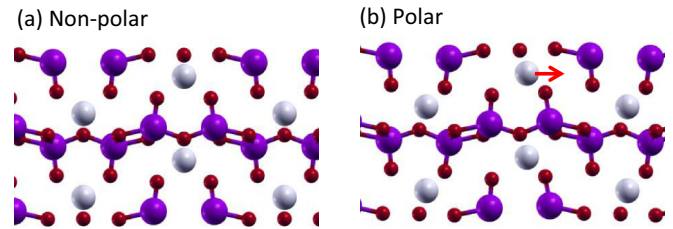
G. LiV_2O_5

LiV_2O_5 consists of layers of V_2O_5 spaced by Li ions, as shown in Fig. 6, and has shown experimental evidence of a phase transition [71]. The ferroelectric polarization is driven by the off-centering of Li atoms. According to PBEsol, the material is nonmagnetic; however, we also examined various magnetic orderings using DFT+U [72–74], with a U value of 3 eV on the V d states. These calculations, which we expect to be more accurate for a material with partially occupied $3d$ orbitals, shows that LiV_2O_5 is a ferromagnetic insulator with a gap of 0.37 eV in the nonpolar phase and 1.00 eV in the polar phase, making LiV_2O_5 a candidate multiferroic. However, the energy difference between the ferromagnetic phase and the lowest energy antiferromagnetic phase is only 2.4 meV/V atom, so the magnetic ordering temperature is likely to be low. LiV_2O_5 is also a potential small band gap ferroelectric.

H. Zn_2BrN, Zn_2ClN, and $AlAgO_2$

Zn_2BrN and Zn_2ClN consist of tetrahedrally coordinated N atoms linked by twofold coordinated Zn, with Br/Cl serving as spacing atoms, as shown in Fig. 7. $AlAgO_2$ shares the same structure, but with AlO_4 tetrahedra spaced by Ag atoms. The polar distortion in these materials consists primarily of a locally nonpolar rotation of the tetrahedra; however, due to the connectivity of the tetrahedra, this results in a polar distortion. The tetrahedra primarily rotate rigidly, and unlike
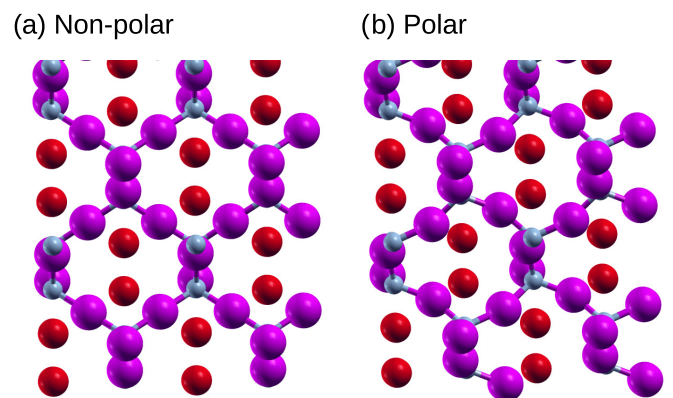

FIG. 7. (a) Nonpolar and (b) polar phases of Zn_2BrN. Polarization is to the left. Small gray atoms are N, magenta atoms are Zn, and red atoms are Br.

$PbAl_2O_4$, which also has rotating tetrahedra, there is no strong off-centering of the atoms in any direction. The result is that even in the case of $AlAgO_2$, where the energy gain from the distortion is substantial, the net polarization is very small. Increasing the polarization in this class of materials would likely require searching for spacing atoms that would couple more strongly to the weakly polar rotation mode, which is reminiscent of the proposed engineering of some improper ferroelectrics [5,75].

IV. CONCLUSIONS

In conclusion, we have performed a high-throughput first-principles search for new ferroelectric compounds. We use two search strategies: (1) starting with known nonpolar structures and looking for polar distortions, and (2) starting with known polar structures and looking for related high-symmetry structures. We discover 16 candidate materials with a variety of interesting properties, including very large polarizations, hyperferroelectricity, antiferroelectricity, and multiferroism. In addition, all the candidates are experimentally synthesized oxides, nitrides, or sulphides, making them likely to be stable under practical conditions, and many of the materials consist of nontoxic and earth abundant elements.

This search uncovers several related classes of materials with similar mechanisms for their polar distortions. We found two materials where the primary polar distortion is due to Li off-centering ($LiScAs_2O_7$, LiV_2O_5), five materials with distortions related to shifting tetrahedral networks (Zn_2BrN, Zn_2ClN, $AlAgO_2$, $PbGa_2O_4$, $PbAl_2O_4$), and four materials that consist of buckling in a layered structure ($SrNb_6O_{16}$, $NaNb_6O_{15}F$, YSF, V_2MoO_8), as well as a few structures with more complicated distortions. Further work will be necessary to understand the full range of properties of these newly discovered ferroelectrics, including the character of the phase transitions of these unusual ferroelectrics and how they couple to strain and other ways of tuning their properties. Nevertheless, we hope that by identifying new classes of materials with energy-lowering polar distortions, we have expanded the universe of materials considered as potential ferrolectrics.

Finally, the high-throughput search techniques used in this work should be applicable to future studies of structural phase transitions.

ACKNOWLEDGMENT

[1] J. W. Bennett, K. F. Garrity, K. M. Rabe, and D. Vanderbilt, Phys. Rev. Lett. **109**, 167602 (2012).

[2] J. W. Bennett, K. F. Garrity, K. M. Rabe, and D. Vanderbilt, Phys. Rev. Lett. **110**, 017603 (2013).

[3] A. Roy, J. W. Bennett, K. M. Rabe, and D. Vanderbilt, Phys. Rev. Lett. **109**, 037602 (2012).

[4] K. F. Garrity, K. M. Rabe, and D. Vanderbilt, Phys. Rev. Lett. **112**, 127601 (2014).

[5] N. A. Benedek and C. J. Fennie, Phys. Rev. Lett. **106**, 107204 (2011).

[6] B. B. Van Aken, T. T. Palstra, A. Filippetti, and N. A. Spaldin, Nat. Mater. **3**, 164 (2004).

[7] C. J. Fennie and K. M. Rabe, Phys. Rev. B **72**, 100103 (2005).

[8] N. A. Benedek, Inorg. Chem. **53**, 3769 (2014).

[9] S. E. Reyes-Lillo, K. F. Garrity, and K. M. Rabe, Phys. Rev. B **90**, 140103 (2014).

[10] C. J. Fennie and K. M. Rabe, Phys. Rev. Lett. **97**, 267602 (2006).

[11] Y. S. Oh, X. Luo, F.-T. Huang, Y. Wang, and S.-W. Cheong, Nat. Mater. **14**, 407 (2015).

[12] J. H. Lee, L. Fang, E. Vlahos, X. Ke, Y. W. Jung, L. F. Kourkoutis, J.-W. Kim, P. J. Ryan, T. Heeg, M. Roeckerath *et al.*, Nature (London) **466**, 954 (2010).

[13] T. Choi, Y. Horibe, H. Yi, Y. Choi, W. Wu, and S.-W. Cheong, Nat. Mater. **9**, 253 (2010).

[14] J. H. Lee and K. M. Rabe, Phys. Rev. Lett. **104**, 207204 (2010).

[15] K. Garrity, A. Kakekhani, A. Kolpak, and S. Ismail-Beigi, Phys. Rev. B **88**, 045401 (2013).

[16] K. Garrity, A. M. Kolpak, S. Ismail-Beigi, and E. I. Altman, Adv. Mater. **22**, 2969 (2010).

[17] S. M. Young and A. M. Rappe, Phys. Rev. Lett. **109**, 116601 (2012).

[18] J. W. Reiner, A. M. Kolpak, Y. Segal, K. F. Garrity, S. Ismail-Beigi, C. H. Ahn, and F. J. Walker, Adv. Mater. **22**, 2919 (2010).

[19] J. Mller, P. Polakowski, S. Mueller, and T. Mikolajick, ECS Journal of Solid State Science and Technology **4**, N30 (2015).

[20] N. A. Hill, J. Phys. Chem. B **104**, 6694 (2000).

[21] A. Jain, G. Hautier, C. J. Moore, S. P. Ong, C. C. Fischer, T. Mueller, K. A. Persson, and G. Ceder, Comput. Mater. Sci. **50**, 2295 (2011).

[22] D. Morgan, G. Ceder, and S. Curtarolo, Meas. Sci. Technol. **16**, 296 (2005).

[23] A. R. Akbarzadeh, V. Ozoli, and C. Wolverton, Adv. Mater. **19**, 3233 (2007).

[24] A. Jain, S. P. Ong, G. Hautier, W. Chen, W. D. Richards, S. Dacek, S. Cholia, D. Gunter, D. Skinner, G. Ceder *et al.*, APL Mater. **1**, 011002 (2013).

[25] S. Curtarolo, W. Setyawan, S. Wang, J. Xue, K. Yang, R. H. Taylor, L. J. Nelson, G. L. Hart, S. Sanvito, M. Buongiorno-Nardelli *et al.*, Comput. Mater. Sci. **58**, 227 (2012).

[26] J. E. Saal, S. Kirklin, M. Aykol, B. Meredig, and C. Wolverton, Jom **65**, 1501 (2013).

[27] P. M. Woodward, Acta Crystallogr. Sect. B **53**, 32 (1997).

[28] P. M. Woodward, Acta Crystallogr. Sect. B **53**, 44 (1997).

[29] C. J. Howard and H. T. Stokes, Acta Crystallogr. Sect. A **61**, 93 (2005).

[30] J. W. Bennett and K. M. Rabe, J. Solid State Chem. **195**, 21 (2012).

[31] J. W. Bennett, Physics Procedia **34**, 14 (2012).

[32] S. C. Abrahams, Acta Crystallogr. Sect. B **44**, 585 (1988).

[33] S. C. Abrahams, Acta Crystallogr. Sect. B **52**, 790 (1996).

[34] S. C. Abrahams, Acta Crystallogr. Sect. B **62**, 26 (2006).

[35] V. Atuchin, B. Kidyarov, and N. Pervukhina, Comput. Mater. Sci. **30**, 411 (2004).

[36] P. S. Halasyamani and K. R. Poeppelmeier, Chem. Mater. **10**, 2753 (1998).

[37] J. W. Bennett, I. Grinberg, P. K. Davies, and A. M. Rappe, Phys. Rev. B **83**, 144112 (2011).

[38] K. F. Garrity, Phys. Rev. B **94**, 045122 (2016).

[39] S. P. Ong, W. D. Richards, A. Jain, G. Hautier, M. Kocher, S. Cholia, D. Gunter, V. L. Chevrier, K. A. Persson, and G. Ceder, Comput. Mater. Sci. **68**, 314 (2013).

[40] See Supplemental Material at http://link.aps.org/supplemental/10.1103/PhysRevB.97.024115 for full structural details of the candidate materials.

[41] P. Hohenberg and W. Kohn, Phys. Rev. **136**, B864 (1964).

[42] W. Kohn and L. Sham, Phys. Rev. **140**, A1133 (1965).

[43] P. Giannozzi *et al.*, J. Phys.: Condens. Matter **21**, 395502 (2009).

[44] D. Vanderbilt, Phys. Rev. B **41**, 7892 (1990).

[45] K. F. Garrity, J. W. Bennett, K. M. Rabe, and D. Vanderbilt, Comput. Mater. Sci. **81**, 446 (2014).

[46] K. F. Garrity, *GBRV Phonon Update and JTH/PSlibrary Testing* (Rutgers University, New Brunswick, 2015).

[47] J. P. Perdew, A. Ruzsinszky, G. I. Csonka, O. A. Vydrov, G. E. Scuseria, L. A. Constantin, X. Zhou, and K. Burke, Phys. Rev. Lett. **100**, 136406 (2008).

[48] S. Baroni, S. de Gironcoli, A. Dal Corso, and P. Giannozzi, Rev. Mod. Phys. **73**, 515 (2001).

[49] R. D. King-Smith and D. Vanderbilt, Phys. Rev. B **47**, 1651 (1993).

[50] K. M. Rabe, *Functional Metal Oxides: New Science and Novel Applications* (Wiley, New York, 2013).

[51] W. Zhong, R. D. King-Smith, and D. Vanderbilt, Phys. Rev. Lett. **72**, 3618 (1994).

[52] R. D. King-Smith and D. Vanderbilt, Phys. Rev. B **49**, 5828 (1994).

[53] O. Diéguez, O. E. González-Vázquez, J. C. Wojdeł, and J. Íñiguez, Phys. Rev. B **83**, 094105 (2011).

[54] Y. Zhou and K. M. Rabe, Phys. Rev. B **89**, 214108 (2014).

[55] Y. Shimakawa, Y. Kubo, Y. Nakagawa, S. Goto, T. Kamiyama, H. Asano, and F. Izumi, Phys. Rev. B **61**, 6559 (2000).

[56] A. Castro, P. Millan, R. Enjalbert, E. Snoeck, and J. Galy, Mater. Res. Bull. **29**, 871 (1994).

[57] B. Marinder, P.-L. Wang, and P. Werner, Acta Chem. Scand. **40**, 467 (1986).

[58] P. Li, X. Ren, G.-C. Guo, and L. He, Scientific Reports **6**, 34085 (2016).

[59] M. Ye, *First-principles Study of Magnetoelectric Effects and Ferroelectricity in Complex Oxides* (Rutgers University, New Brunswick, 2016).

[60] T. Schleid and Z. Anorg. Allg. Chem. **625**, 1700 (1999).

[61] G. V. Kozlov, A. A. Volkov, J. F. Scott, G. E. Feldkamp, and J. Petzelt, Phys. Rev. B **28**, 255 (1983).

[62] A. K. Tagantsev, Ferroelectrics **79**, 57 (1988).

[63] T. F. Krüger and Hk. Müller-Buschbaum, J. Alloys Compd. **190**, L1 (1992).

[64] J. P. Perdew and A. Zunger, Phys. Rev. B **23**, 5048 (1981).

[65] K.-B. Plötz and Hk. Müller-Buschbaum, Z. Anorg. Allg. Chem. **488**, 38 (1982).

[66] G. Henkelman, B. P. Uberuaga, and H. Jónsson, J. Chem. Phys. **113**, 9901 (2000).

[67] P. Mahe-Paillert, Rev. Chim. Miner. **7**, 807 (1970).

[68] K. Y. Yun, D. Ricinschi, T. Kanashima, M. Noda, and M. Okuyama, Jpn. J. Appl. Phys. **43**, L647 (2004).

[69] P. Pailleret, J. Borensztajn, W. Freundlich, and A. Rimsky, C. R. Hebd. Seances Acad. Sci. **263**, 1131 (1966).

[70] H. A. Eick and L. Kihlborg, Acta Chem. Scand. **20**, 722 (1966).

[71] J. Galy, C. Satto, P. Sciau, and P. Millet, J. Solid State Chem. **146**, 129 (1999).

[72] V. I. Anisimov, J. Zaanen, and O. K. Andersen, Phys. Rev. B **44**, 943 (1991).

[73] S. L. Dudarev, G. A. Botton, S. Y. Savrasov, C. J. Humphreys, and A. P. Sutton, Phys. Rev. B **57**, 1505 (1998).

[74] M. Cococcioni and S. de Gironcoli, Phys. Rev. B **71**, 035105 (2005).

[75] A. T. Mulder, N. A. Benedek, J. M. Rondinelli, and C. J. Fennie, Adv. Funct. Mater. **23**, 4810 (2013).